Chapter V

EXPERIMENTAL RESULTS AND DISCUSSION

5.1 Introduction

The aims of the experiment work were (1) to determine the microstructure of the various sensitization specimens by scanning electron microscopy (SEM); (2) to verify the degree of sensitization leading to the susceptibility to stress corrosion cracking (SCC) in type 304 stainless steel using slow strain rate tensile (SSRT) test technique; and (3) to provide a quantitative technique for characterizing DBPA spectrum. Integration of these tasks will result in a complete description and application of the new quantitative technique for identifying the susceptibility to SCC in type 304 austenitic stainless steel.

5.2 Experimental Results and Discussion

5.2.1 Determination of the Microstructure of the Specimens

The etched specimens were examined in a scanning electron microscope (SEM) to determine their microstructures. The variations of the microstructures of the etched specimens with sensitization time are shown in figure 5.1. The grain size of the specimens was found by line-intercepting method and was determined to be 11-μm. It should be noted that even after 16-hours of sensitization no grain growth is detected.

Figure 5.1(a) Micrograph show the carbides precipitate along grain boundaries for 0-hour sensitization.

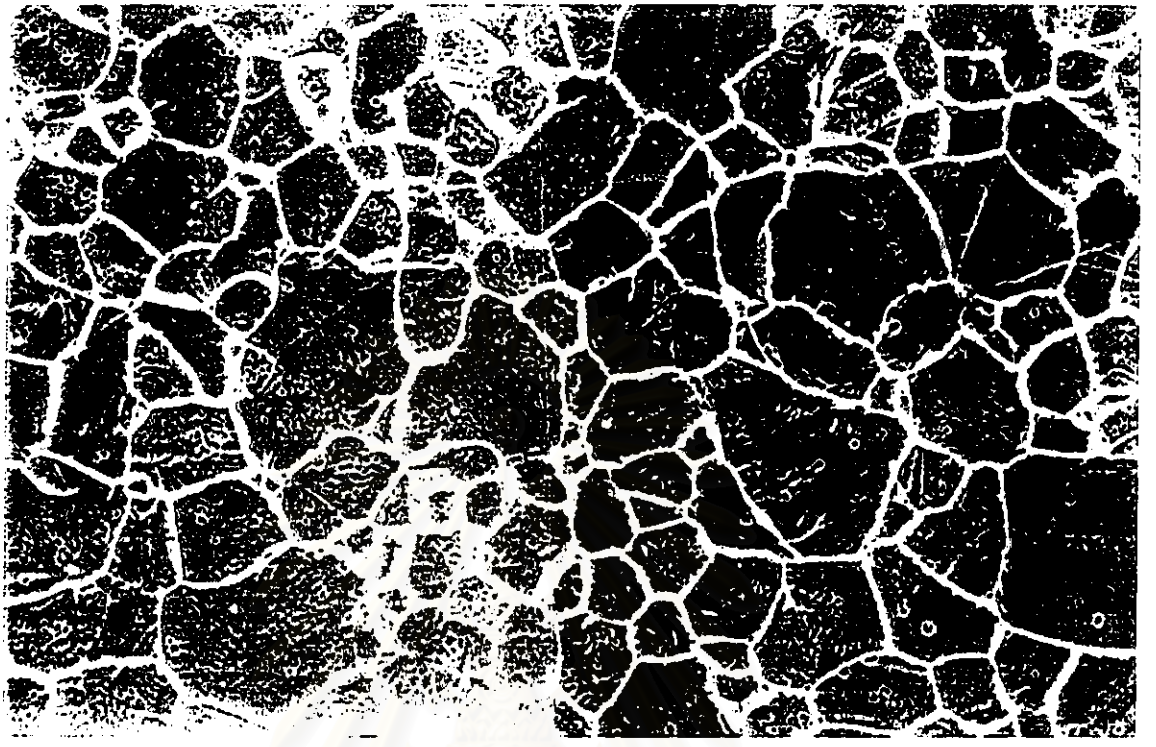

Figure 5.1(b) Micrograph show the cabides precipitate along grain boundaries for 8-hour sensitization.

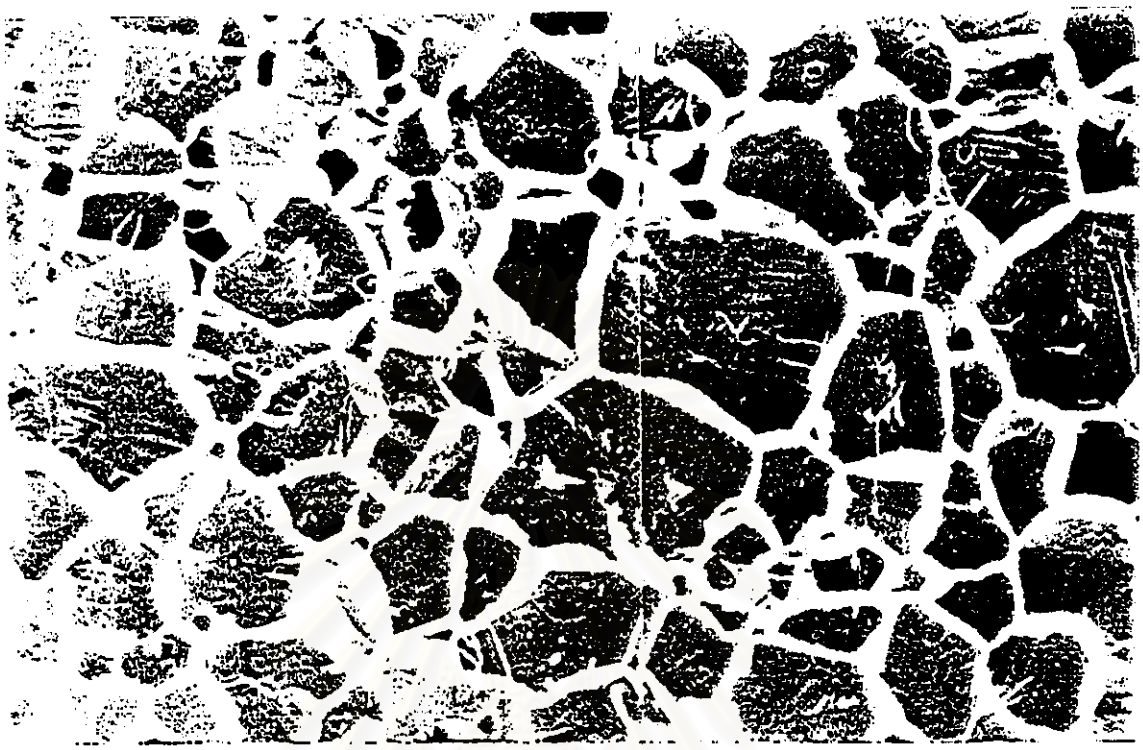

Figure 5.1(c) Micrograph show the carbides precipitate along grain boundaries for 16-hour sensitization.

After oxalic acid etched, degrees of sensitization were estimated by measuring the area and thickness of carbides that cover grain boundaries. Figure 5.1 shows scanning electron micrograph of specimens after oxalic etched. The relationship between grain boundary carbide areas and sensitization times is shown in figure 5.2. As expected, there is no carbide in the solution annealed specimens while the 8-hours and 16-hours sensitized specimens was moderately and heavily covered by the carbides, respectively.

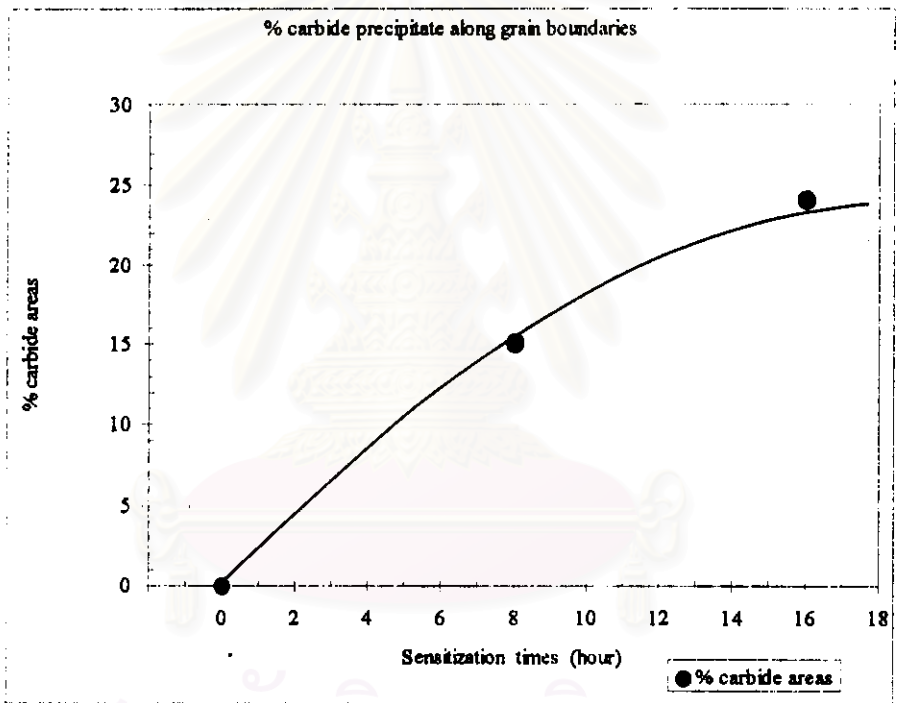

Figure 5.2 Shows the relationship between attacked grain boundary carbide areas and sensitization time.

According to figure 5.1, the etched specimens show a higher sensitization level at 8-hours and 16-hours. Microstructure resulting from etching indicated the sensitized grain boundaries increased with increasing sensitization time at a given temperature. This was described by the fact that the tendency to carbide precipitation

shows considerable boundary-to-boundary variation [44, 45]. According to Bennet and Pickering, grain boundary with lower boundary energy requires a longer sensitization time before carbide precipitation occurs [46]. Thus, short sensitization time causes precipitation and chromium depletion occurred only on a small proportion of grain boundaries. These boundaries are attacked during etching by oxalic acid. Longer sensitization times cause precipitation to occur on less favorable grain boundary so that the total length of grain boundary attack increases. The width of depleted zone was also found to increase with increasing sensitization time in etching test.

D.B. Wells et al. [47] studied the use of percolation theory to predict the probability of failure of sensitized austenitic stainless steel by IGSCC. It was found that the material with less than 23% of sensitized grain boundaries would not fail by IGSCC. The material with between 23% and 89% of sensitized grain boundaries will show mixed ductile tearing and brittle failure in a slow strain rate tensile test, and the material with more than 89% sensitized grain boundaries will show only brittle intergranular failure. The typical ductile tearing compared to SCC brittle failures in stainless steel are shown in figure 5.3. The form of percolation used to simulate the sensitized grain boundaries is called bond percolation. The material is model as 3D dimensional structure of bonds, which represent grain boundaries. Each bond can be "inactive" i.e., not sensitized, or "active", i.e., sensitized grain, from a linked of vulnerable, chromium-depleted material across the facet. As the percentage of "active" bond" is increased, the network or cluster size increase. An analysis of the relationship between the percentage of active bonds in the structure and the predicted distribution of the cluster sizes determined the degrees of sensitization of that structure to intergranular failure. As a result, figure 5.4 illustrates of linked grain boundaries (percentage of sensitized grain boundaries) versus heat treatment time (650° C). Figure 5.5 shows the relationship between percentage of grain boundary carbides area as measured from our micrograph and the percentage of linked grain boundaries for various sensitization times. It also was clear from the figure that for a given sensitization time, percentage of grain boundary carbide areas correlates with percentage of linked grain boundaries.

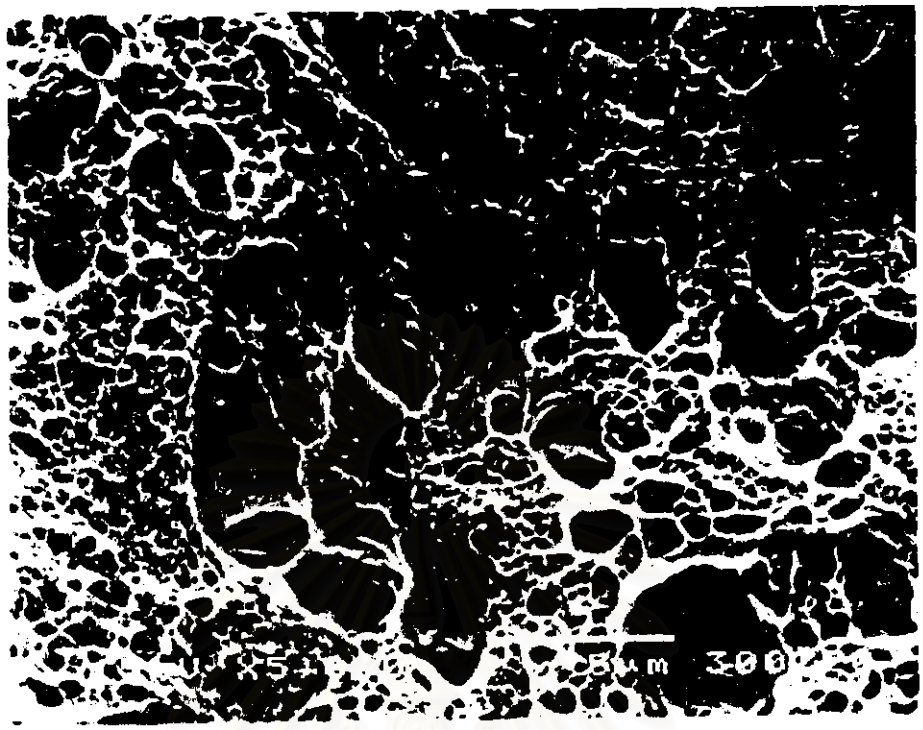

(a)

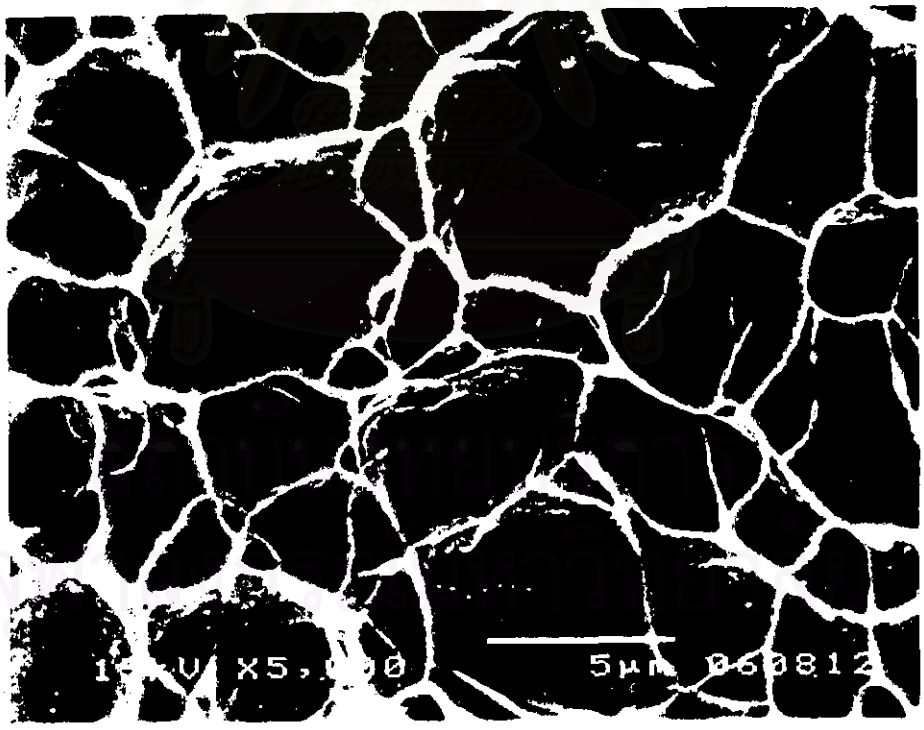

(b)

Figure 5.3 Illustration of the typical ductile over load failure (a) and stress corrosion cracking failure(b).

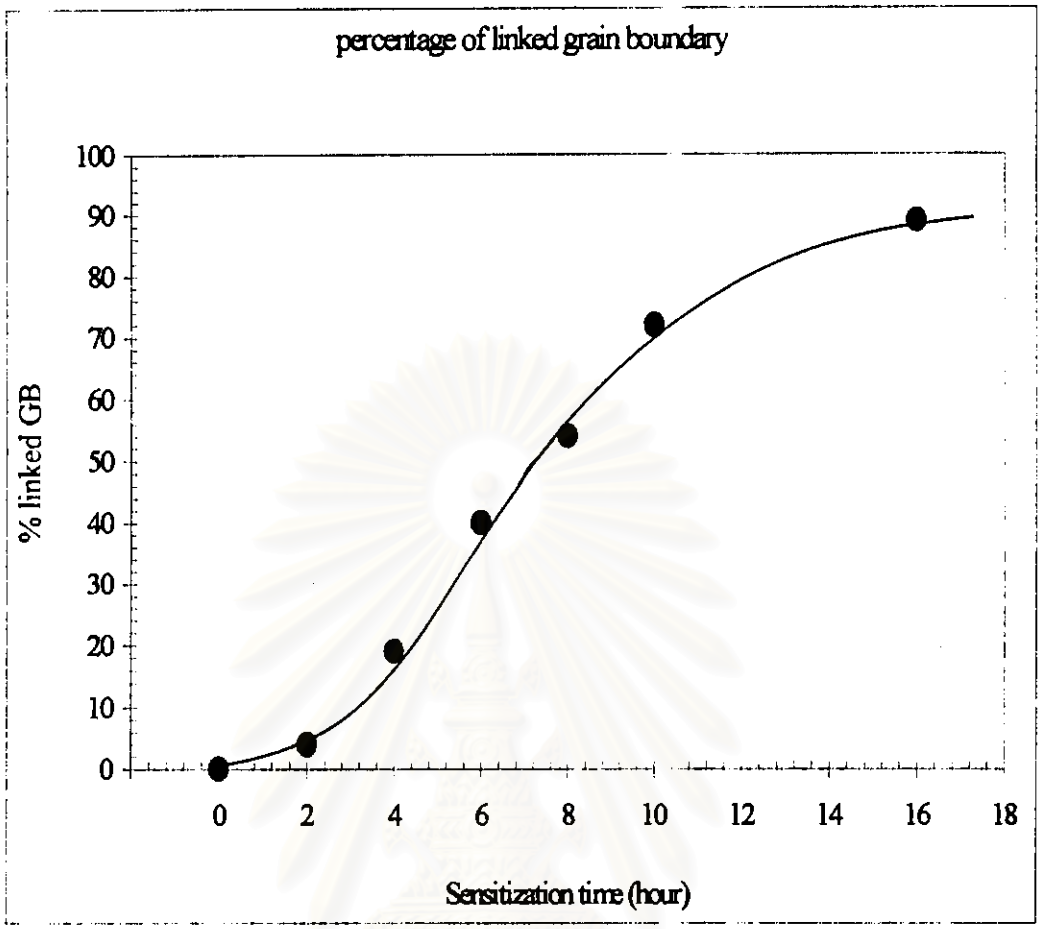

Figure 5.4 The relationship between percentage of linked grain boundaries-vs-heat treatment time (at 650° C).

When the change in percentage of linked grain boundaries of the various sensitization times was plotted together with the percentage of grain boundaries carbide areas, figure 5.6, a linear correlation between percentage of the areas of carbides that cover grain boundaries and percentage of linked grain boundaries was observed.

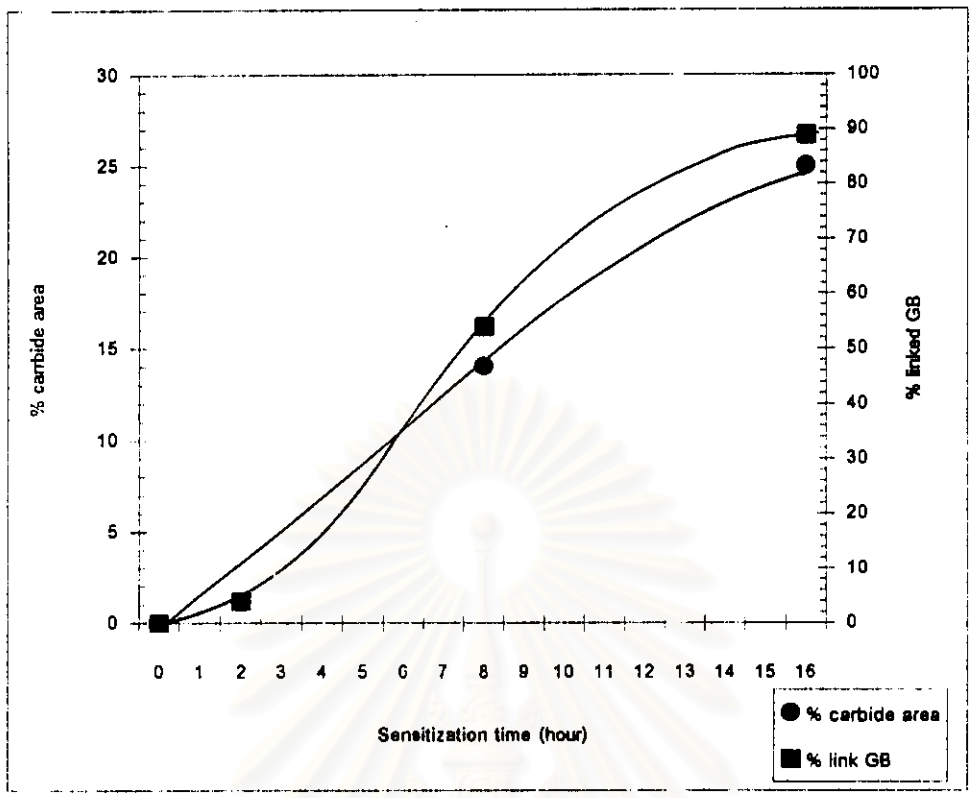

Figure 5.5 Illustration of the relationship between percentage of grain boundary carbide areas and percentage of linked grain boundaries for various sensitization time.

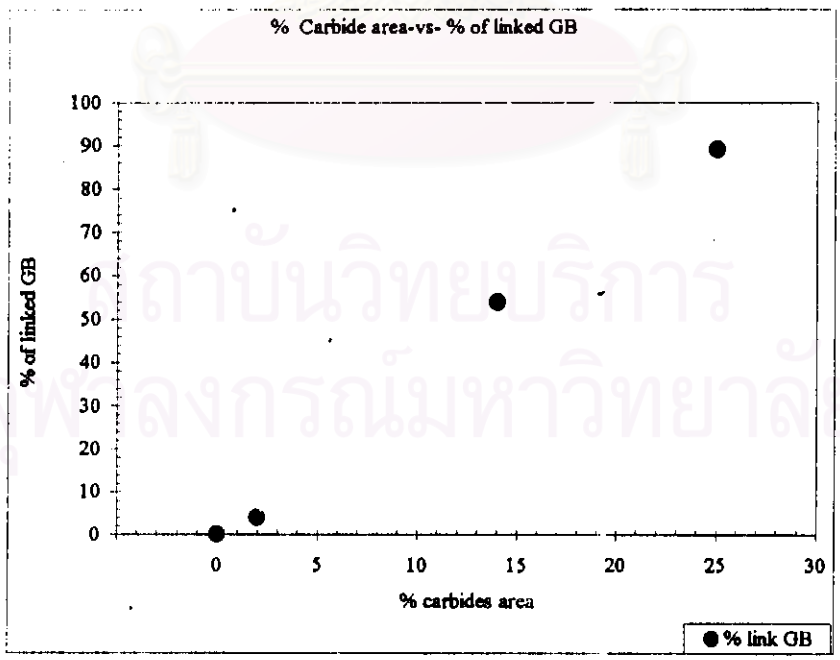

Figure 5.6 Illustration of the relationship between percentage of carbide areas and percentage of linked grain boundaries.

5.2.2 Determination of the IGSCC Susceptibility

Figure 5.7 presents engineering stress-vs-engineering strain curves of various sensitized specimens tested in 0.5-M thiosulfate solution. A significant drop in strength occurred in sensitized specimens. A large drop in maximum load indicated poor resistance to SCC. This behavior was related directly to susceptibility to SCC of the specimens.

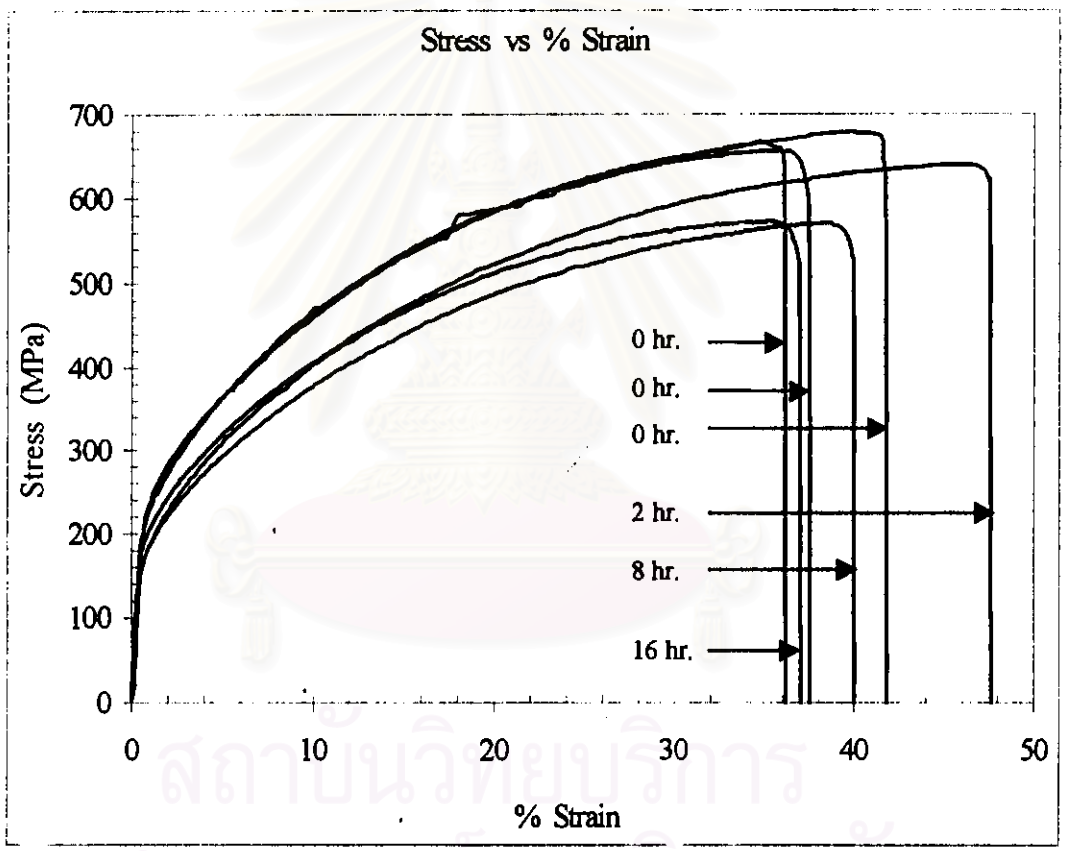

Figure 5.7 The engineering stress-vs-percentage of engineering strain for various sensitized specimens test in 0.5-M sodium thiosulfate at ambient temperature.

From figure 5.7, we can determined the ultimate tensile strength (UTS), which is the stress corresponding to the maximum load applied to the specimens, of various sensitized specimens as shown in table 5.1.

Table 5.1 The summary of results obtained from the SSRT test.

Sensitization time (hour)	UTS (Mpa)	Failure mode
0	662*	Ductile
2	636	SCC
8	567	SCC
16	566	SCC

* Obtained from the average.

From table 5.1, the UTS of the solution annealed were found to be 662, 673 and 653-MPa and the average of them was 662-MPa. The UTS of the specimens sensitized at 2-hour showed the UTS of 636-MPa. The specimens sensitized at 650° C for 8 to 16-hour showed lower UTS of 567 and 566-MPa, respectively. Figure 5.8 illustrates the relationship between the UTS of the sensitized specimens and sensitization time. Apparently, the UTS of the various sensitized specimens decrease when the sensitization time increase while the strains to failure were not significant altered.

The least susceptibility to SCC was observed when the sensitization time was 0-hour (solution annealed) followed by 2-hour, 8-hour and 16-hour. This indicates the level of the chromium depletion in the grain boundary zones had a significant influence on IGSCC susceptibility of the sensitized stainless steel. The chromium content near grain boundary decreases with increasing sensitization time as shown in figure 5.9. A decrease in chromium content of the depleted zones at grain boundary causes a decrease in the effectiveness of the passive film and increases the chemical activity of the region. According to the anodic dissolution mechanism, the experimental conditions present the susceptibility to SCC. The above considerations suggest a mechanism of anodic dissolution of chromium depleted zones under the

influence of tensile stress. Thus, it was assumed that if the extent of chromium depletion at grain boundary was very high, then IGSCC initiation was possible at very low values of plastic strain because of the increased chemical activity to depleted zones.

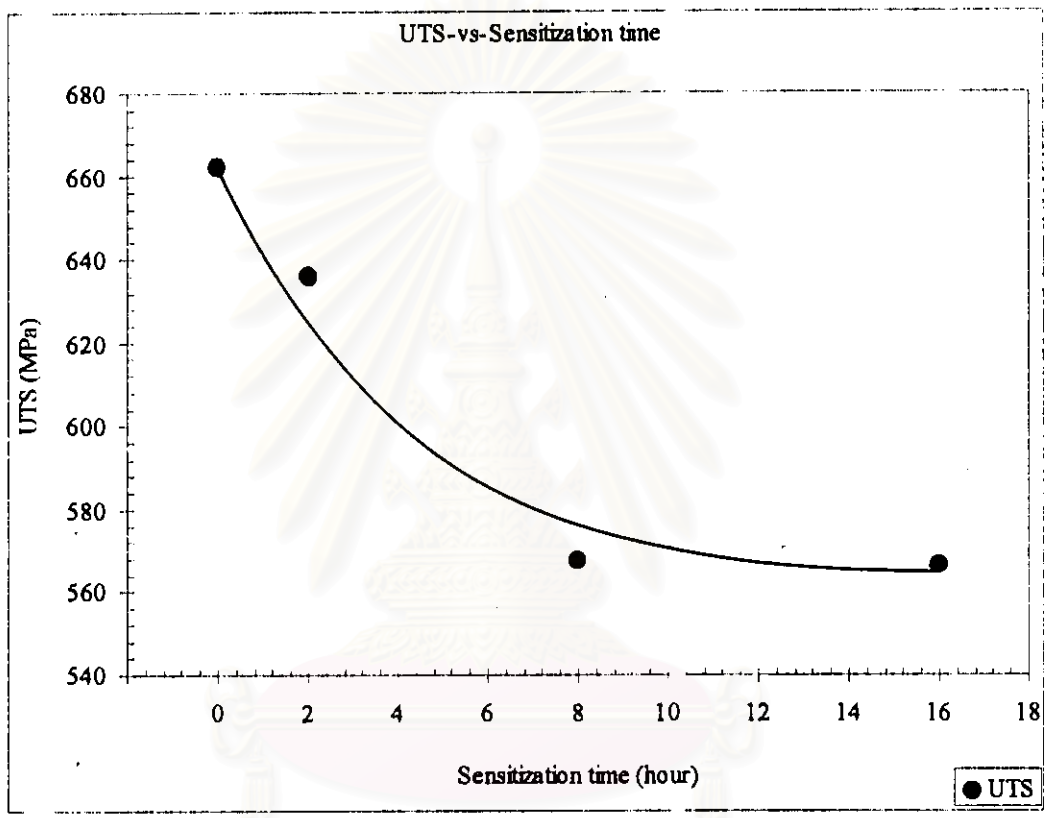

Figure 5.8 Illustration of the relationship between the ultimate tensile strength (UTS) of the specimens and sensitization time.

High magnification SEM photographs of the fracture surface of the sensitized specimens are illustrated in figure 5.10 (a) through (d). The solution annealed shows mostly ductile tearing in the fracture surface. As expected, a higher sensitization level at 8-hour and 16-hour showed entirely brittle failure with only small amount of ductile tearing in isolated plane. A summary of the SSRT results such as sensitization time, the UTS of the various specimens and mode of failure is presented in table 5.1.

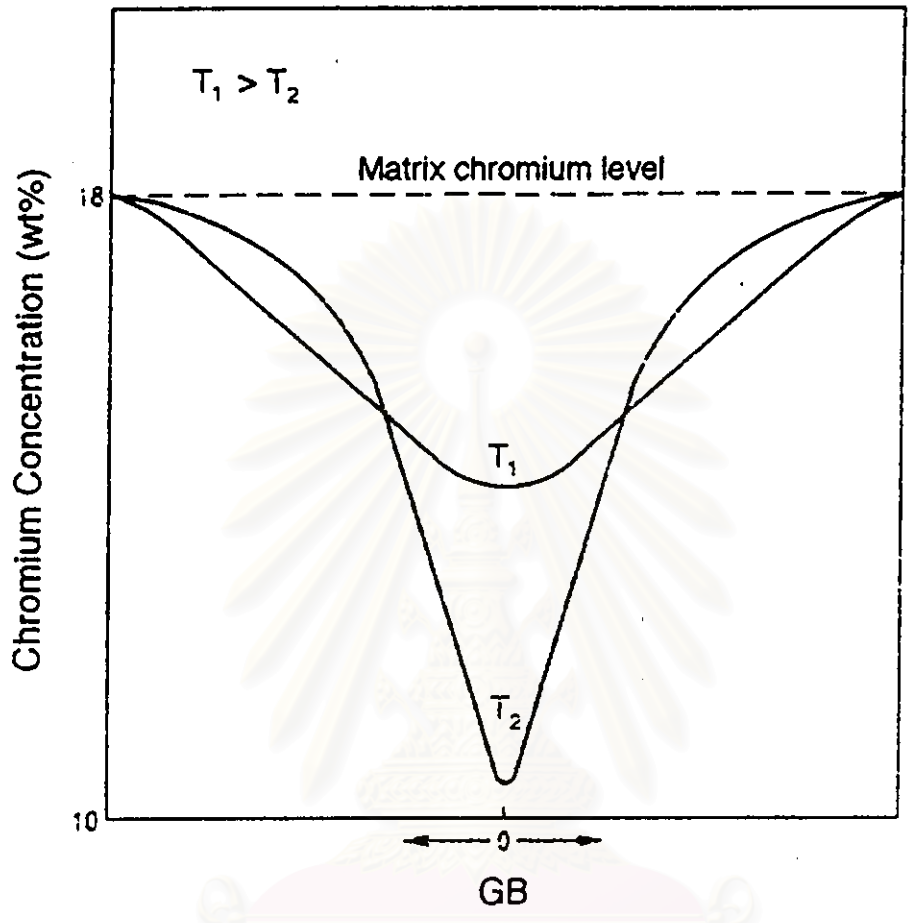

Figure 5.9 Schematic of chromium-depletion profiles at two times.

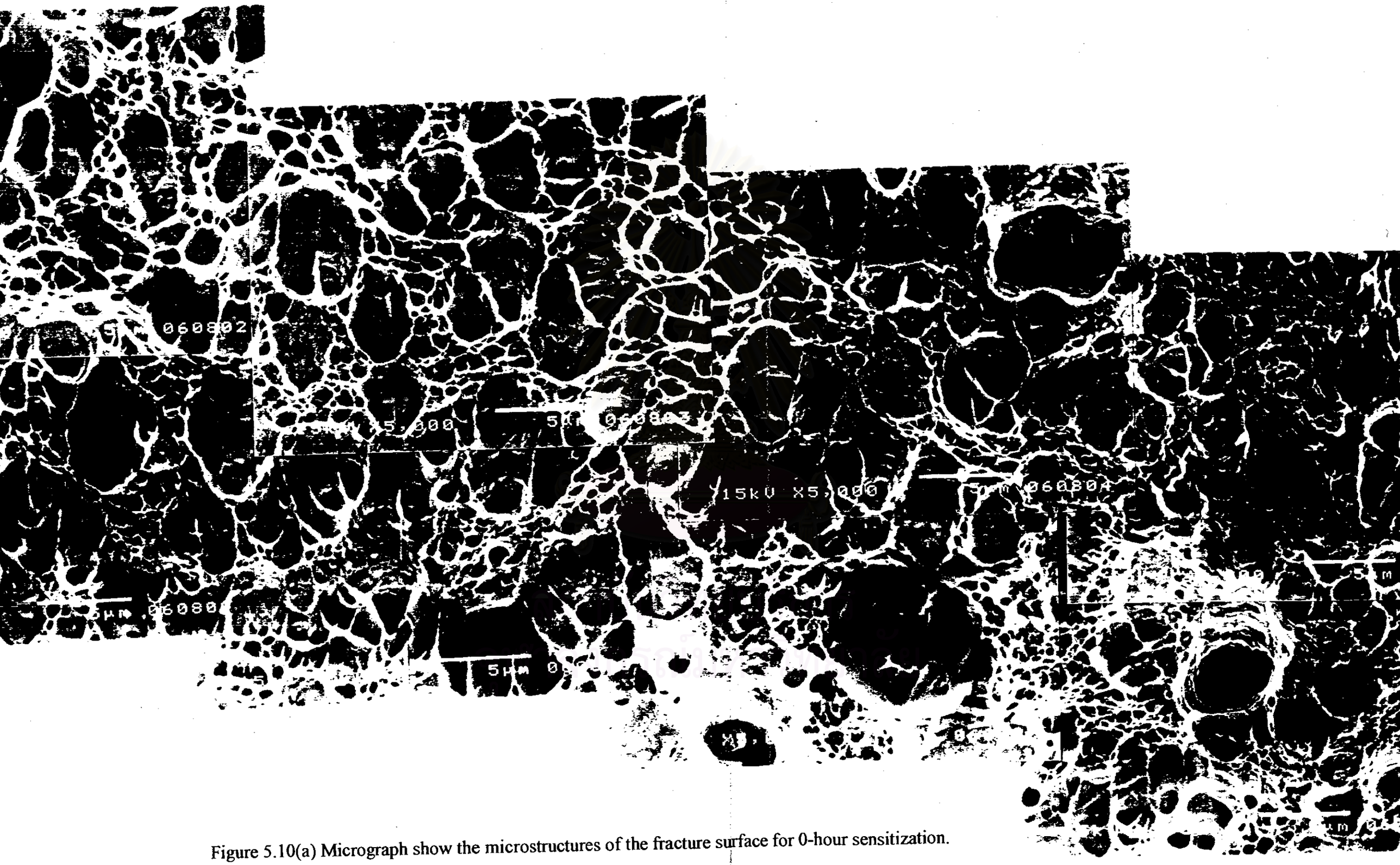

Figure 5.10(a) Micrograph show the microstructures of the fracture surface for 0-hour sensitization.

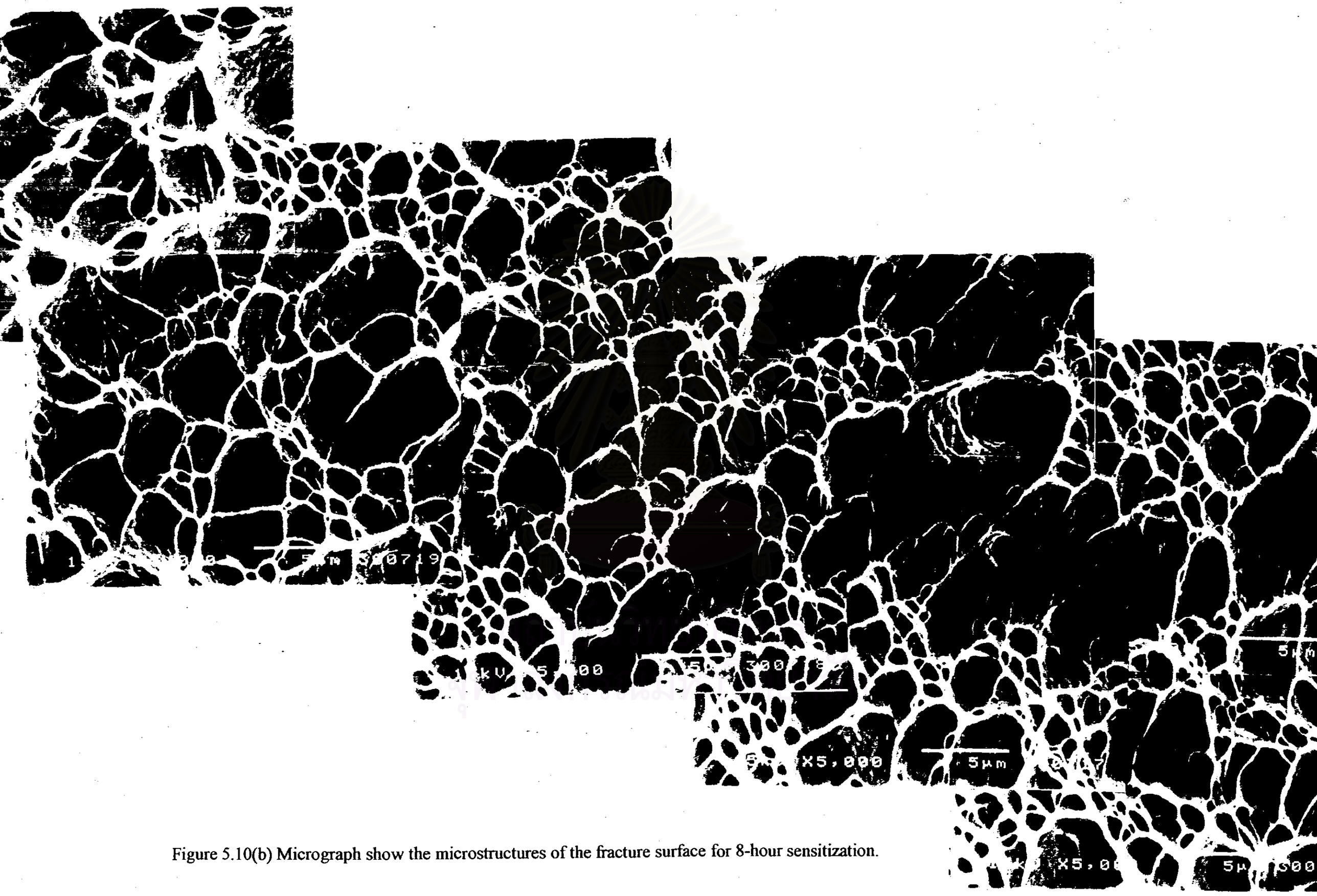

Figure 5.10(b) Micrograph show the microstructures of the fracture surface for 8-hour sensitization.

Figure 5.10(c) Micrograph show the microstructures of the fracture surface for 16-hour sensitization.

Based on the above mentioned, the mechanism, which is responsible for SCC in thiosulfate solution, may be view as following;

In general, IGSCC susceptibility of sensitized specimens increase with heat treatment time for a given temperature. This result was in accordance with the anodic dissolution mechanism for SCC because the extent of chromium depletion increases with the sensitization time, making the grain boundaries more anodic and more susceptible to SCC. The schematic of anodic dissolution mechanism of SCC growth is shown in figure 5.11. This event has been observed in the sensitized specimens because of the formation of relatively low wide chromium-depleted zones with low level of depletion.

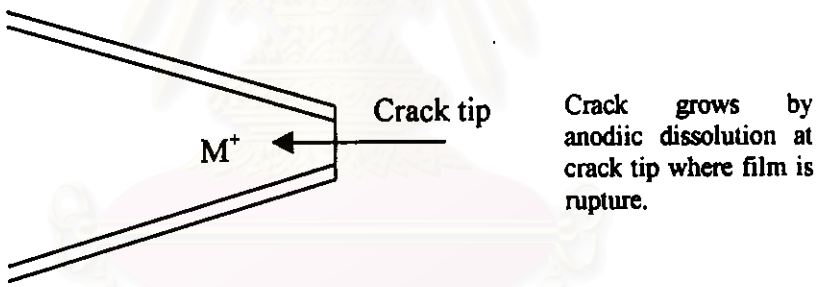

Figure 5.11 Illustration of the schematic summary of anodic dissolution mechanism.

According to figure 5.10, it also was clear that the smooth fracture surface has been observed in sensitized specimens while the ductile overload failure has been observed in solution annealed specimen. Thus, it is believed that the process of repeated film rupture is an essential part of the SCC process. The typical schematic diagram of anodic dissolution SCC and ductile overload failure has been shown in figure 5.12.

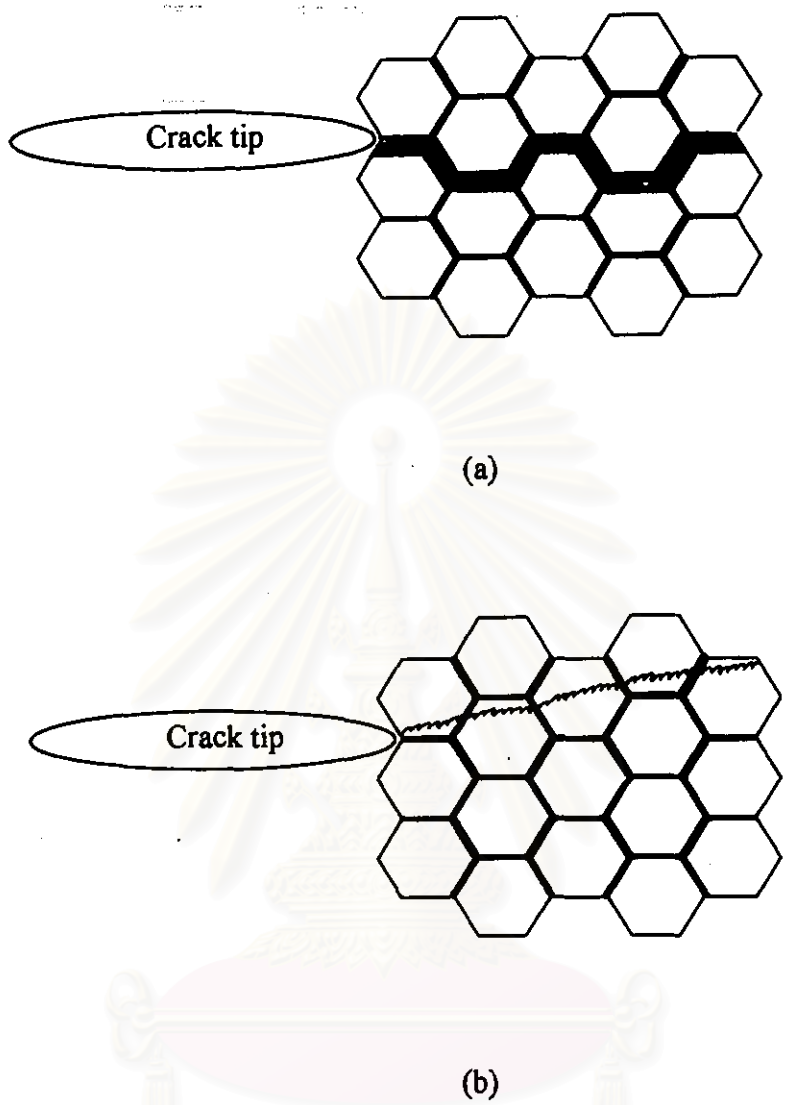

Figure 5.12 Illustration of the schematic diagram of anodic dissolution SCC (a) and ductile overload failure (b).

Film rupture or slip-step dissolution [45] was one of the first proposed SCC mechanisms and still receives considerable support. Tensile stress is assumed to produce sufficient strain to rupture the surface film at an emerging slip band, and a crack grows by anodic dissolution of the unfilmed surface at the rupture site. Film rupture is essentially caused by the transfer of strain from the based metal to the film. It should be noted that local conditions conductive to metal dissolution are generated

while repassivation begin and limits the amount of dissolution. The dissolution and repassivation taken together may be considered as an oxidation process [46].

5.3 Correlation of the S parameter, Degree of Sensitization with SCC Susceptibility

The decrease in the UTS of sensitized specimens is directly related to the precipitation of chromium carbides or chromium depletion at the grain boundary. It is clear that the UTS decrease when the carbides precipitate along grain boundary increase. When the change in UTS of the various sensitized specimens is plotted together with the ΔS value obtained from DBPA spectroscopy [40], figure 5.13. It was clear from the figure 5.13 that the S parameter increases with increasing sensitization time. While the UTS decrease with increasing sensitization time. This indicated that the S parameter is inversely related to the degree of embrittlement in stainless steels under testing conditions. Therefore, it may be concluded that it was possible to estimate the susceptibility to SCC of type 304 stainless steel by measuring DBPA spectroscopy.

5.4 Conclusion

1. By using SSRT test, the UTS of the specimens decrease while sensitization time increases. Thus, the least susceptibility to SCC of the specimen test in 0.5-M sodium thiosulfate solution was observed when the sensitization time increased.

2. A new method for determining the susceptibility of type 304 austenitic stainless steels to stress corrosion cracking has been established based on DBPA spectroscopy.

3.For a given sensitizing temperature, there was a good correlation between the S parameter obtained from DBPA spectroscopy and the susceptibility to SCC.

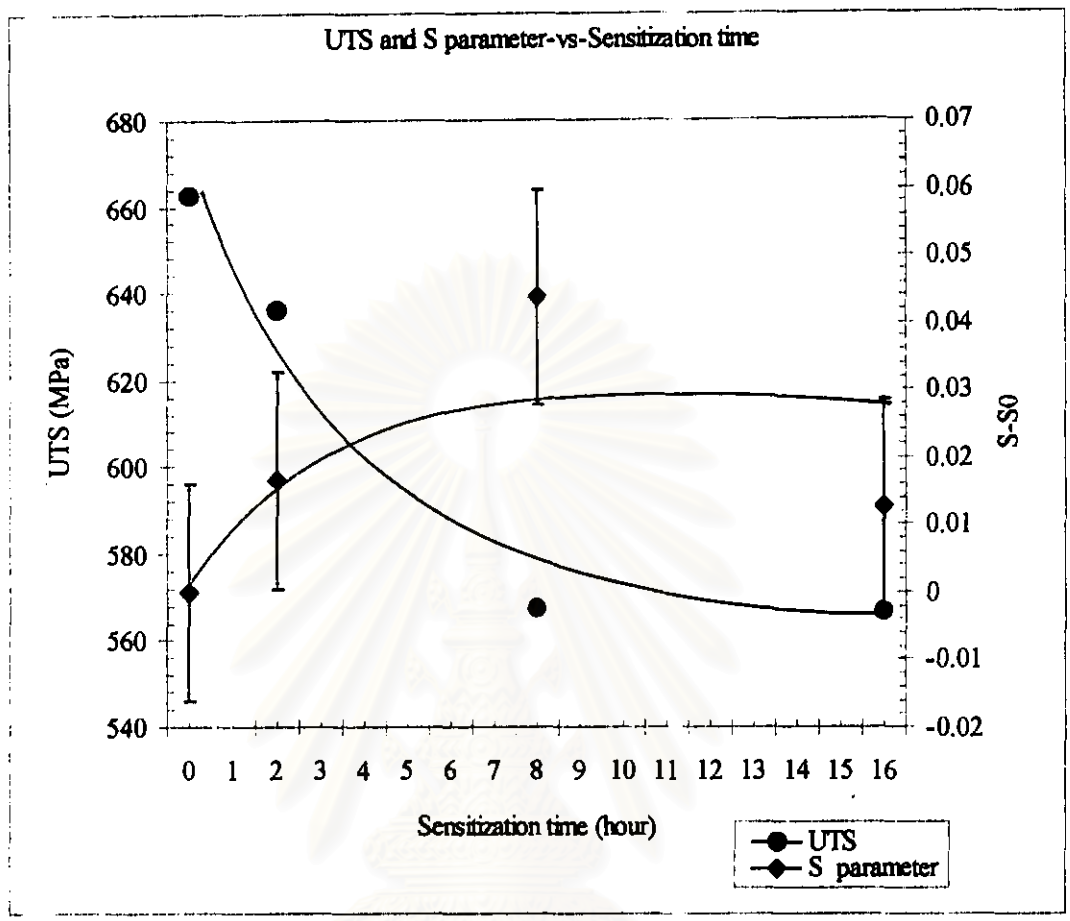

Figure 5.13 Illustration of the relationship between UTS, change in the S parameter for various sensitization time.